Nicotine and Tobacco Research, 2025, **27**, 1499–1512
https://doi.org/10.1093/ntr/ntaf062
Advance access publication date 11 March 2025
Review

Continuous Nicotine Monitors for Personal Nicotine Pharmacokinetics: A Receptor-Aware Research Agenda

Aaron L. Nichols PhD[1], Christopher B. Marotta PhD[2], Heather Lukas PhD[3], Nicholas J. Friesenhahn BS[2], Daniel A. Wagenaar PhD[1], Stephen L. Mayo PhD[1], Dennis A. Dougherty PhD[2], Neal L. Benowitz MD[4], Wei Gao PhD[3], Anand K. Muthusamy PhD[1,2,5], Henry A. Lester PhD[1]

[1]Division of Biology and Biological Engineering, California Institute of Technology, Pasadena, CA, USA
[2]Division of Chemistry and Chemical Engineering, California Institute of Technology, Pasadena, CA, USA
[3]Andrew and Peggy Cherng Department of Medical Engineering, Division of Engineering and Applied Science, California Institute of Technology, Pasadena, CA, USA
[4]Division of Cardiology, Department of Medicine, University of California, San Francisco, CA, USA
[5]Convergent Research, Inc., Cambridge, MA, USA

Corresponding Author: Henry A. Lester, PhD, Division of Biology and Biological Engineering, California Institute of Technology, 1200 E. California Blvd., Pasadena, CA 91125, USA. Telephone: +1 626-395-4946; E-mail: lester@caltech.edu

Abstract

A minimally invasive "continuous nicotine monitor" (CNM) would resolve the dynamic nicotine concentration, *[nicotine]*$_t$, faced by high-sensitivity nicotinic acetylcholine receptors (nAChRs) during and after nicotine intake by individual subjects. Motivations: "Know the potential enemy at an individual level." Smoking or vaping produces an initial "bolus" of nicotine in the blood and brain, lasting ~5 minutes with a peak concentration of ~100–200 nM. The bolus largely governs reinforcement, reward, and cognitive enhancement. A prolonged declining phase of [nicotine], with a half-time of 1–4 hours, largely suppresses withdrawal symptoms and governs the known cell biology of addiction. Next, "Know the potential therapy," because individual *[nicotine]*$_t$ records will be useful during research on the effectiveness of nicotine replacement therapy. Finally, "Know the physiology." The only three known effects on nAChRs in cerebrospinal fluid at the relevant *[nicotine]*$_t$ are activation, desensitization, and chaperoning/upregulation. Therefore, additional mechanistic insights will arise from correlating *[nicotine]*$_t$ with readily measurable physiological data on those effects in molecular, cellular, and brain slice systems and animal models. Interstitial fluid is the appropriate compartment for a CNM. The molecular sensor technology could employ fluorescence, as shown by progress on measuring *[nicotine]*$_t$ with improved variants of intensity-based nicotine-sensing fluorescent reporters (iNicSnFRs). Electrochemical measurements of *[nicotine]*$_t$ may also be possible. Studies like the Population Assessment of Tobacco Health would contextualize *[nicotine]*$_t$ measurements during each subject's ad libitum nicotine intake, hopefully at a cost <$100 for a 24-hour record.

Implications

We propose the first research agenda leading to a wearable continuous nicotine monitor (CNM). We explain that this interdisciplinary agenda must be publicly funded and not-for-profit. The CNM would measure the time-varying concentration, *[nicotine]*$_t$, experienced by nicotinic receptors. We define the challenging specifications for a CNM, and we show how present techniques can nearly meet these challenges. With the appropriate CNM, individual *[nicotine]*$_t$ can be measured in populations of 10,000 or more subjects, addressing many present and future hypotheses about individual nicotine pharmacokinetics and receptor physiology for all modes of human nicotine intake, including emerging nicotine replacement therapies.

Introduction

Ever since Columbus's crew sampled tobacco in 1492, nicotine research has led the way in new concepts and techniques for neuroscience. With that history in mind, we intend this article to inform two communities. The *nicotine and tobacco research community* may wish to learn about the prospects for new generations of wearable, minimally invasive or non-invasive devices to measure the pharmacokinetics of nicotine at an individual level.

The *wearable device community* may wish to learn about the specific opportunities and challenges associated with nicotine. The opportunities are great: at any given time, some 60% of the world's >1 billion smokers would like to quit. The challenge: nicotine is present at concentrations ~ 1 million times smaller than glucose, the target for the most successful continuous, minimally invasive monitor, yet the required time resolution resembles that for glucose!

We wish to measure nicotine concentration *[nicotine]* versus *time*, *t*, near the relevant receptors, or *[nicotine]*$_t$. Since tobacco produces primarily the S-enantiomer and only the charged species binds to nicotinic acetylcholine receptors (nAChRs), one would more precisely write *[(S)-nicotine$^+$]*$_t$.

Received: October 22, 2024. Revised: February 17, 2025. Accepted: March 3 2025.

Three Motivations for the Proposed Continuous Nicotine Monitor

1."Know the Potential Enemy": Personal Pharmacokinetics

It is already known that cigarettes and electronic nicotine delivery systems (ENDS) produce two phases of *[nicotine]*$_t$. The first phase occurs while nicotine is entering the blood. It is the *relatively high, initial peak or* "bolus" of [nicotine] (100–200 nM for 5–10 minutes, Figure 1, area highlighted mins 0–10). This phase appears to provide reinforcement via a sense of well-being, stress relief, or cognitive boost. The bolus results from the efficiency of smoking/vaping: (1) the large area (50–75 m^2) of the lungs and (2) the high membrane permeability of the nicotine free base. During a puff, nicotine crosses the apical and basolateral membranes of alveolar endothelial cells, reaching arterial blood within a few seconds, then the brain a few seconds later.[3–6] When nicotine is no longer present in the alveoli, *[nicotine]*$_t$ begins to decline.

Oral nicotine products (ONPs) include nicotine pouches, lozenges, gums, and inhalers and involve permeation through the buccal tissues rather than the alveoli. Transdermal patches eponymously use transfer through the skin.

The *prolonged, declining phase* of *[nicotine]*$_t$ (Figure 1, area highlighted mins 10–60) occurs with a half-time of 1–4 hours after a single cigarette. The prolonged phase both suppresses withdrawal symptoms and maintains the cellular biological aspects of addiction.[7] For a given individual, the prolonged declining phase probably differs less than the bolus among methods of intake, because the flux of nicotine into the blood and cerebrospinal fluid (CSF) has nearly stopped. An exception is the transdermal patch; after removal, there may be a plateau of 1–2 hours before the decline begins.

Within a given study (15–30 subjects), *[nicotine]*$_t$ measured with a single method of nicotine intake shows great variability among subjects; a typical coefficient of variation (CV) is at least 0.5.[8] When nicotine is administered intravenously in controlled doses (mg/kg), the CV is usually much smaller.[8] The variability in *[nicotine]*$_t$ among users is a strong reason to study individual *[nicotine]*$_t$ records. Experiments will require orders of magnitude more subjects than is possible with existing pharmacokinetic methods to address open problems in addiction and therapy:

1. Pioneering studies suggest that menthol prolongs the lifetime of [nicotine] in mice[9] and humans,[10] increases conditioned place preference to nicotine in mice,[11] and potentiates upregulation of nAChRs in mice and humans (see "Know the Physiology," below).[12] Menthol might exert these effects via (1) its inhibition of cytochrome P450 2A6 (CYP2A6),[13] (2) its inhibition of TrpA1 channels in respiratory pathways,[14] or (3) its action as a chemical chaperone for nAChRs.[11] Mechanism (1), but neither (2) nor (3), would increase and prolong *[nicotine]*$_t$.
2. On average, women experience more difficulty in smoking cessation than men.[15–17] Experiments with deuterium-labeled nicotine show that the prolonged declining phase is faster in women.[18] Men seem to value the reinforcing effects of the bolus more than women[15]; Does this arise from sex differences in the bolus? How extensive are the individual variations? Does estrogen accelerate nicotine metabolism solely by inducing CYP2A6[18]?
3. Do the varied effects of nicotine across the lifespan[19] correlate with changes in nicotine pharmacokinetics, for instance slowed pharmacokinetics in elderly people[20,21]?

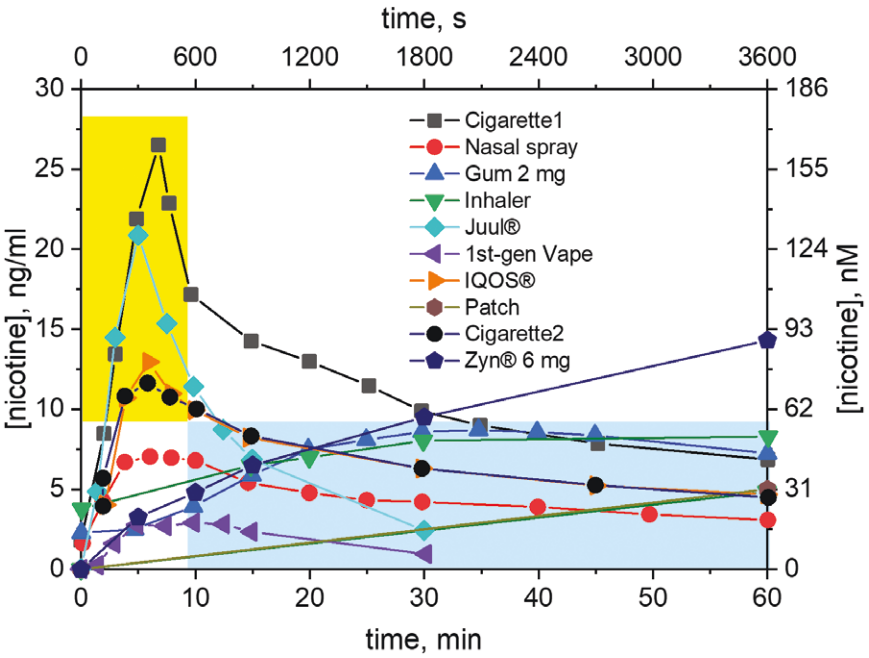

Figure 1. Collected data on time course of plasma *[nicotine]*$_t$ using the intravenous (IV) blood-draw method. Measurements on cigarette smoking cover a wide range, mostly falling between the two examples given (Cigarette1[1] and Cigarette2[2]). Juul, Cigarette1, first-generation (pre-2015) vape[1]; IQOS, Cigarette2[2]; Nasal spray, Gum, Inhaler, Patch[118]; Zyn.[119] Time zero is the first puff, insertion of the pouch, or attachment of the patch. Measures of variability have been omitted for clarity. All studies comprised at least 24 subjects at least 19 y of age. In one study,[2] the subjects had an average age of 34 y and were 52.5% male. Study[118] is a review that compiled several other studies. Two studies[1,119] did not report on average age or % male.

4. Do smokers titrate the bolus to achieve 100–150 nM nicotine, but no more?
5. How does the bolus change with reduced-nicotine cigarettes[22–24] or adjustable e-cigarettes[25]?
6. How do individual vapers control $[nicotine]_t$ during the day? Do some "seek the peak" and others "avoid the trough?"

2."Know the Potential Therapy": Personal Nicotine Replacement Therapy

Nicotine replacement therapy (NRT) will play a role in smoking cessation for the foreseeable future. Various national regulatory agencies (for instance, the US Food and Drug Administration [FDA]) have *approved* nicotine for smoking cessation via NRT in the form of transdermal patches, inhalers, and gum.

This *approval* does not yet extend to ENDS, which now receive *authorization* for marketing from the FDA's Center for Tobacco Products (CTP) as "reduced risk products" (RRPs) under the Tobacco Control Act of 2009. Like many previous authors, we acknowledge the potential abuse liability of RRPs, including the possibility that RRPs could cause increases in dual use (vaping and smoking).[26]

However, the FDA's Center for Drug Evaluation and Research (CDER) has now cleared at least one "investigative new drug" (IND) application of an ENDS for investigation as a prescription-only device leading to smoking cessation. In an early iteration of the rationale for such devices, previous CTP and FDA leaders stated,[27] "We are examining possible steps the agency could take to address the pharmacokinetic performance of FDA-approved medicinal nicotine products to help more smokers quit. Factors for consideration may include the speed with which nicotine is delivered... [from] products capable of delivering nicotine without having to set tobacco on fire." In a promising technology, piezoelectrically driven ultrasonic mesh inhalers produce controllable droplet size, require no carrier molecules such as propylene glycol and vegetable glycerin, and do not heat the liquid at all.[28,29] This could represent a step forward in individually controllable NRT.[30–32] The mesh nebulizer that received the IND clearance showed $[nicotine]_t$ kinetics approaching that of a cigarette and much faster than a conventional inhaler.[33]

Several metrics have been proposed as guidelines for effective NRT. One suggestion is to measure flux from the device to the subject[34]; this can be measured in the device itself or by collecting nicotine with an impactor. A continuous nicotine monitor (CNM) measuring $[nicotine]_t$ near the relevant nAChRs would be much more useful by capturing the best time resolution. It has been suggested[35] that the most successful means of smoking cessation involves the greatest rate of rise of $[nicotine]_t$, $\frac{d[nicotine_t]}{dt}$,presumably duplicating the "bolus." An aspirational CNM must resolve the bolus, on an individual basis.

Newer techniques for delivering NRT also raise the specter of abuse liability in two ways. First, it must be noted that many individuals fail to quit smoking with buccal or transdermal NRT because they miss the bolus from a cigarette. If a prescription-only device, such as an ultrasonic nebulizer, perfectly copies the bolus of a user's favorite cigarette, after a prescribed time course of NRT, a smoker might simply switch to a nicotine salt ENDS, which does optimize the bolus. We acknowledge that vaping manufacturers could use a CNM to enhance the bolus and, therefore, increase abuse liability.

Second, nicotine may well remain in the CSF for the prolonged declining phase, desensitizing nAChRs and provoking the cell biology of nicotine addiction. Newer ONPs also have abuse liability.

Despite these concerns about the abuse liability of NRT, one cannot deduce either the bolus or the prolonged declining phase during therapeutic NRT from first principles; we must perform dynamic, quantitative, individual measurements of $[nicotine]_t$. Individual measurements of $[nicotine]_t$ are a highly appropriate component of research to test hypotheses that various forms of NRT benefit distinct subgroups of people defined by "tobacco abuse."[36]

3."Know the Physiology": Activation, Desensitization, and Chaperoning/Upregulation of Receptors

The CNM concept interfaces directly with nearly a century of research on time-resolved nAChR responses. Nicotine acts on nAChRs in only three ways, according to present knowledge. Nicotine activates nAChRs, producing ion flux (including Ca^{2+} flux) and depolarization. After a few minutes at the relevant nAChRs, nicotine desensitizes nAChRs. Slowest of all—hours to days—nicotine upregulates nAChRs via one or more post-translational processes, primarily chaperoning of nascent nAChRs within the endoplasmic reticulum (ER). The first two processes have received intense study since the identification of nAChRs, including experiments on isolated cells, brain slices, in vivo recordings on animal models, imaging of nAChR availability, functional magnetic resonance imaging, and heterologous expression, mostly via electrophysiological and Ca^{2+} recording.

Chaperoning/upregulation are both more complex and less well studied.[7,37–41] How is the prolonged phase crucial for nicotine dependence? Nicotine enters the ER, beginning a pathway that we term "inside-out."[7] This entry occurs within a few seconds after nicotine appears near cells, and at a concentration within 2-fold of the extracellular value.[42] Importantly, even [nicotine] as low as 10 nM activates the "inside-out" pathway,[40] and in some people, [nicotine] continues to exceed 10 nM for ~6 hours after smoking/vaping.[42–46] A major effect of the inside-out pathway is to produce upregulation of plasma membrane nAChRs, and this upregulation is selective at every level studied—brain region, cell type, axonal versus somatic versus dendritic localization, and subunit stoichiometry of the upregulation nAChRs.[7]

Important simplifications are now in hand: It is generally agreed that the relevant nAChRs are α4β2*, α6β2*, and possibly α2β2* (the * denotes the possible presence of an additional subunit, such as α5, in the assembled pentameric receptor). Also, the relevant peak $[nicotine]_t$ values are those achieved by smoking, <200 nM, in part because higher *[nicotine]* activates other nAChRs in aversive pathways. In another major simplification, measurements in CSF are unnecessary: nicotine reaches the CSF within seconds from brain capillaries because of its high $logD_{pH7.4}$.[47]

Some aspects of nicotine pharmacokinetics are shaped by the effects of inhaled nicotine in the mouth, airways, and the alveolar epithelium; the nicotine concentrations in these compartments are much higher than considered above, and they take place at additional targets. (1) Deprotonated (free base) nicotine activates TrpA1, a channel abundantly expressed in airways.[14,48] This irritation could induce "braking" of respiration.[49] (2) Aerosolized nicotine in the alveoli equilibrates with the cytosol of alveolar epithelial

cells, and this could lead to cytosolic concentrations of hundreds of millimolar (mM; Henry's law). In alveolar epithelial cells, these concentrations may be high enough to chaperone and upregulate additional nAChRs, such as α3β4*.[50,51] These complications are additional reasons to measure *[nicotine]*$_t$ in CSF-like compartments, downstream from measurements on nicotine flux from devices.

The CNM Concept Is Directly Relevant to Social and Behavioral Studies of Nicotine Intake

Because nicotine consumption—certainly for the abusive aspects, and probably also for the smoking cessation aspects—involves many cues, social support, and other activities such as eating and drinking, flavorings, and diurnal rhythms, it is crucial that measurements of *[nicotine]*$_t$ occur during ad libitum consumption in daily life. The CNM we envision would satisfy this requirement.

The Population Assessment of Tobacco Health (PATH) study has resulted in 737 research papers as of mid-2024. The PATH study's biomarker and biospecimen components have varied. PATH-like studies would be enhanced by 24-hour CNM records of *[nicotine]*$_t$, and we argue below that such records would be more useful than the currently employed urinary nicotine equivalents. Distributing and supporting the CNM could become as straightforward as the activities associated with continuous glucose monitors (CGMs; see below). If a study also collects tissue, blood, or saliva, the DNA analyses could further define additional components of nicotine metabolism, including CYP2B6[52] and CYP2E1.[53]

Present Measurements of *[nicotine]*$_t$

The classical ideas introduced so far have motivated measurements of *[nicotine]*$_t$ on hundreds of subjects gathered in several recent reviews.[8,35,54] Two methods now provide "gold standard" measurements of nicotine pharmacokinetics. The intravenous blood-draw method is performed in a clinic on a subject with an intravenous catheter.[1,2,55–57] It costs thousands of dollars per subject, including tens of dollars for each sample in a typical series of 10–25 samples repeated at 5-minute intervals. The positron emission tomography (PET) method, which mixes ^{11}C-nicotine with inhaled smoking or vaping, has a better temporal resolution (a few seconds).[58,59] For both methods, a study typically includes 15–30 subjects. Both methods are too tedious and expensive for routine personal use. Neither can be routinely applied to youths.

Slower methods have been especially useful in showing that the prolonged, declining phase varies up to 10-fold among individuals, partially due to polymorphisms in cytochrome P450 2A6 (CYP2A6). CYP2A6 partially governs the conversion of nicotine to (nearly inactive) cotinine.[60] The "nicotine metabolite ratio" (NMR) measures CYP2A6 activity. NMR reveals that ~15% of the population are "slow" metabolizers: individuals with defective CYP2A6 have up to a severalfold longer [nicotine] half-life, and the increase depends on the genotype.[60] Slow metabolizers smoke fewer cigarettes per day; but especially for moderate to heaving smokers, they score just as strongly "dependent" on Fagerstrom-like tests.[61]

NMR does not measure the key data stream, *[nicotine]*$_t$. Furthermore, genetic risk scores capture only 34.5% of the variability in NMR.[62,63] Proxy measures for *[nicotine]*$_t$ in blood include urinary nicotine metabolites. The only presently available physiological proxy for *[nicotine]*$_t$, increased heart rate,[45] is complicated for ad libitum intake because heart rate is influenced by several activities of daily living: exercise, simultaneous consumption of caffeinated beverages and nicotine, and tolerance to subsequent cigarettes.[64–66] Some ENDS measure puff strength, duration, and frequency ("smoking topography").[67]

Thus, *[nicotine]*$_t$ is the relevant metric and conventional intravenous (IV) and PET methods have too few subjects to resolve most confounding factors. In contrast, we envision a CNM that costs <100 USD (2024) to scalably study tens of thousands of subjects, transforming "confounding factors" for either therapy or abuse into "identifiable risk factors" or "personal smoking cessation therapy."

Relationship to Conventional Pharmacological Concepts

Unbound Concentrations

All the techniques we envision will monitor the *unbound concentration of nicotine*$^+$. This is the form sensed by the binding site of nAChRs, the active site of enzymes such as CYP2A6, and the binding site of biosensor proteins described below. However, the TrpA1 channel probably binds the deprotonated (free base) form.[14]

Volume of Distribution

The unbound concentration of any drug should be distinguished from the total amount of the drug in the organism.[68] This concept is usually associated with apparent volume of distribution. Volume of distribution in humans is conventionally inferred from measurements of the so-called clearance.[68] Most drugs have an apparent volume of distribution >1 L/kg, thought to arise either via drug binding to proteins, accumulation within lipids, or accumulation within acidic organelles ("acid trapping"). Nicotine has a relatively low volume of distribution, 1.8–4.2 L/kg,[69] with a consensus value of 2.6 L/kg.[70] That is, nicotine becomes bound or otherwise sequestered to the extent that the total amount of nicotine in the body would be appropriate to the volume of water equal to ~2.6 times the body's weight ("corporal water volume").

Most of these possibilities and mechanisms can influence *[nicotine]*$_t$. Therefore, some of these mechanisms would shape the data stream produced by a CNM—but none would challenge the validity of the *[nicotine]*$_t$ data as they apply to actions on nAChRs.

Area Under the Curve of Concentration ×Time

Area under the curve (AUC) is often invoked to compare actions of therapeutic drugs. For nicotine, abuse potential is sometimes assumed to increase with AUC,[54,71,72] but this idea has little experimental proof. More generally, the goal to "know the physiology" will transcend the AUC metric by showing how the bolus and the prolonged phase affect activation, desensitization, or chaperoning of nAChRs.

Interstitial Fluid Is the Most Relevant Compartment

CSF bathes highly nicotine-sensitive nAChRs in several distinct brain regions; therefore, *[nicotine]*$_t$ in CSF governs activation, desensitization, and upregulation of nAChRs. However, no minimally invasive or noninvasive, nonradioactive

technique is available for measuring $[nicotine]_t$ in CSF. For all means of nicotine intake, the blood–brain barrier, formed by tight junctions in cerebral capillaries and by the end-feet of astrocytes, provides a delay of at most a few seconds in achieving a CSF $[nicotine]_t$ that essentially equals blood $[nicotine]_t$.[8,47]

As in most organs, brain cells lie within 50 μm of capillaries. Nicotine can diffuse passively over 50 μm within 5 seconds (assuming a diffusion constant of 0.5 μm^2/ms). Smokers and vapers feel a "buzz" within ~20 seconds, showing that nicotine has appeared in the CSF and reached nAChRs. Rat measurements confirm that $[nicotine]_t$ in CSF is close to that in plasma.[73] Special intra-arterial [^{11}C]nicotine PET measurements in humans achieve a resolution of ~5 seconds,[4,6,58] which is unnecessary for most studies of $[nicotine]_t$.

Interstitial fluid (ISF) is minimally invasive. Nicotine is predicted to be slightly more permeable to capillaries in peripheral tissue than to brain capillaries; but the difference is likely to be just a few seconds. In this context, time-resolved measurements of $[nicotine]_t$ in ISF are presumably more relevant than blood to $[nicotine]_t$ in CSF.

Commercial tobacco manufacturers modify the taste and and/or pH of cigars and cigarettes; and this may also modify $[nicotine]_t$.[74,75] In nicotine salt ENDS, the pH of the e-liquid and of the aerosol is lower than cigarettes; but the higher solubility of nicotine$^+$ than of free base nicotine allows increased [nicotine$^+$] in the e-liquid and in the inhaled aerosol. Manufacturers of nicotine salt ENDS may also choose an anion that affects airway flow.[6,76] All NRT strategies also manipulate nicotine pharmacokinetics.[8,35]

On the one hand, the various effects on nicotine entry into the blood cannot yet be predicted simply either from the amount of e-liquid left in the reservoir, from the volume of each puff, or from the nicotine deposited on an impactor after a controlled number of mechanical puffs. On the other hand, once the nicotine enters the blood, its concentration (<1 μM) is so low that buffers in the blood maintain its pH at ~7.4. If a nicotine salt is ingested, the blood similarly dilutes the anion, which therefore need not be considered further. As noted above, the nicotine passes within seconds from the blood to the CSF and other compartments such as ISF. Therefore, $[nicotine]_t$ in the blood or ISF is an excellent measurement of the delivery system's total pharmacologically relevant, dynamic result—whether the delivery system is a combustible cigarette, an ENDS, an ONP, or NRT.

In summary, we strongly favor interstitial fluid as the compartment of choice for measurements of personal $[nicotine]_t$.

Analogy to CGMs

All FDA-approved CGMs reside in ISF, are inserted with minimally invasive techniques, transmit their data, $[glucose]_t$, wirelessly, and have a temporal resolution of ~5 minutes. One FDA-approved glucose monitor uses fluorescent detection,[77,78] although via a different molecular mechanism than the one described below.

Most CGMs now in use employ electrochemical detection via glucose oxidase positioned at the intradermal tip of a 5-mm-long gold wire. The latest electrochemical CGMs last ≥10 days. CGMs have become commodity items, available over the counter ($50) for use by prediabetic patients and by nondiabetic consumers to satisfy their curiosity about their $[glucose]_t$. Several labs are now attempting to develop CGMs in essentially noninvasive form: arrays of microneedles a few hundred micrometers long and tens of micrometers wide, with their tips in ISF.

Sweat

Although sweat measurements have the great advantage of being noninvasive, other aspects lead to uncertainties that sweat can provide quantitative, time-resolved measurements relevant to CSF. Sweat is secreted through a complex duct at varying pressures. According to a biofluidic model of sweat glands, a biomolecule secreted by the gland reaches the skin surface within <5 minutes, fulfilling the temporal resolution criterion of a CNM.[79] Active microfluidics may then be required in the sensor device to transport the sweat to the sensing surface or chamber. This would introduce a delay; but if the flow is laminar, the time of actual secretion can be determined.[80] Primary sweat (in the sweat coil) is quite acidic,[79] leading to concerns about acid trapping, which may explain initial measurements that [nicotine] in sweat is >10 times higher than in blood.[81] It is not understood whether the walls of the sweat duct would then allow reabsorption of nicotine. Researchers in the sweat sensor field are working to eliminate these complications, with the goal of realistic measurements on a known time scale.[82–85]

Specifications for a CNM

Concentration Resolution: ~10 nM

Although the EC_{50} for nicotine activation of nAChRs is typically several hundred nanomolar (nM), much lower concentrations desensitize or upregulate nAChRs.[7] For instance, the EC_{50} for upregulation is 37 nM.[40] We therefore consider it necessary to measure $[nicotine]_t$ as it declines to values as low as ~10 nM.

Absolute [Nicotine] Calibration

The signal from all copies of the CNM should have an invariant, simple relationship to $[nicotine]_t$. In Figure 2, we show that a candidate fluorescent sensor molecule displays a linear response in the relevant range of [nicotine], and we refer to the sensitivity as δ-slope. We would accept an absolute accuracy of ±20%. Modern electrochemical CGMs do have absolute calibrations, in part because a few CGMs from each production batch are tested at varying [glucose]; the resulting calibrations are then embedded in all CGMs from the batch.[87]

Temporal Resolution: 5 Minutes

The CNM must have the temporal resolution to measure the bolus of $[nicotine]_t$ (~100 nM for ~5 minutes, Figure 1, area highlighted mins 0–10). This implies a temporal resolution of ~300 seconds: the typical 10-puff period for a single cigarette or a typical ENDS "vaping session." Juul and IQOS achieve 60–150 nM nicotine during this 300- to 600-second time frame (Figure 1).

Selectivity: At Least 100-Fold for Nicotine

The ideal CNM would have zero response to other molecules in the ISF. We aim to render the sensing molecules 100-fold more sensitive to nicotine than to all other ligands. According to this specification, even if an endogenous interfering molecule has a 100-fold higher concentration higher than nicotine, this would not markedly distort the $[nicotine]_t$ signal.

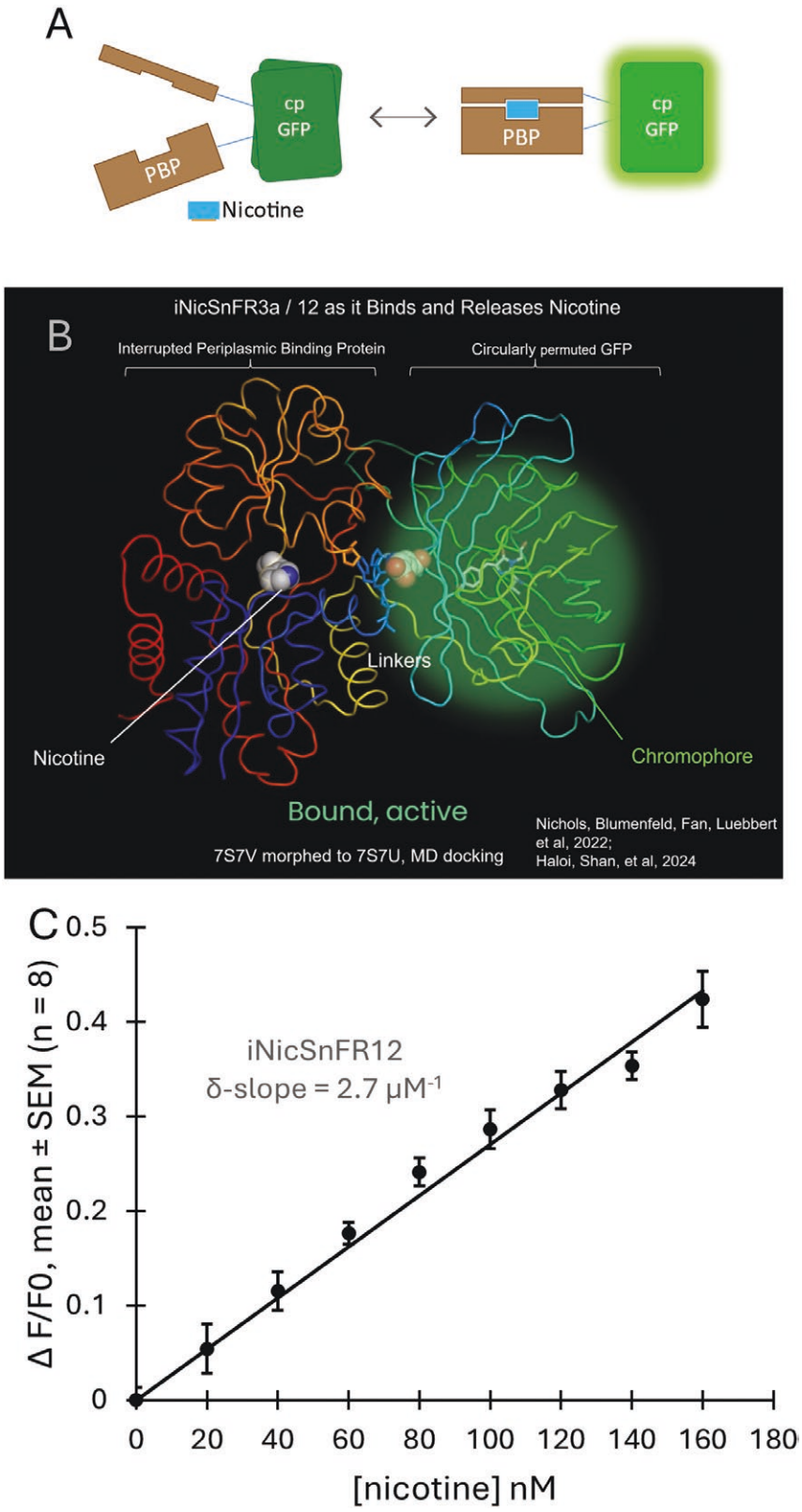

Figure 2. Molecular basis of the iNicSnFR approach to a CNM. A, Schematic view of the single-chain fluorescent sensing molecule such as iNicSnFR12. B, A single frame from Supplementary Video S1, depicting the details of the conformational change that underlies sensing of nicotine by iNicSnFR12. C, Concentration–response curve at [nicotine] in the range 0–180 nM, the expected plasma, CSF, or ISF range during nicotine intake via smoking, vaping, transdermal patches, inhalers, or oral nicotine products.[8] Measurements were conducted in 96-well microtiter plates, and each well contained 100 nM purified iNicSnFR12 in 100 μL of solution. F_0 and ΔF are the resting fluorescence and additional nicotine-induced fluorescence, respectively. The excitation and emissions wavelengths are 496 and 535 nm, respectively. From Haloi et al.[86] CSF = cerebrospinal fluid; CNM = continuous nicotine monitor; iNicSnFR = intensity-based nicotine-sensing fluorescent reporter; ISF = interstitial fluid.

Durability: At Least 24 Hours

A suitable first-generation CNM would measure $[nicotine]_t$ for roughly 24 hours. This would allow 40 or more cigarettes or vaping sessions, providing an excellent view of the prolonged phase. Including a full 24 hours has the additional advantage that $[nicotine]_t$ is expected to fall to nearly zero during the night, providing an important set of control readings.

Measurements of $[nicotine]_t$ during research on smoking cessation would require much longer records. By analogy with CGMs, a 10-day period seems approachable. Mice with brain expression of cpGFP-based biosensors provide signals for as long as 1 year.[88] Mice expressing an adeno-associated virus encoding iFentanylSnFR, which differs by only a dozen amino acids from intensity-based nicotine-sensing fluorescent reports (iNicSnFRs), continue to give useful responses to fentanyl for at least 3 weeks.[89]

Available Molecular Technology for a CNM

Nicotine-Binding Protein-Based Approaches: The iNicSnFR Family

The iNicSnFR family[42,86,90] is based on ~50 years of research on periplasmic binding proteins (PBPs), comprising some 20 000 genes in bacterial and archaeal species. The PBP binds a small molecule (ligand) of importance to the microorganism (in an intact bacterium, the PBP would then present the ligand to other proteins). More than 450 atomic-scale structures for PBPs now exist in the protein data bank RCSB. In all known cases, the PBP responds to the ligand binding by undergoing a conserved "Venus flytrap" or "clamshell" conformational change.[91] Most known PBPs exist as monomers, and the conformational change depends on the ligand conformation with a Hill coefficient near 1. This well-understood change requires <1 second in most cases, rendering the PBP suitable to become the molecular basis of a real-time, continuous, reversible, reagent-less sensor (Figure 2).

The PBP of most interest for a CNM is a mutated variant of OpuBC from a hyperthermophilic bacterial species which uses choline or betaine as an osmolyte. We mutated OpuBC to favor binding of acetylcholine[92] or nicotine.[42] Each member of the iNicSnFR family is a single protein chain. The chain represents a nearly modular merger of two moieties: the PBP binding moiety and a fluorescent readout moiety. We use the term "merged" to avoid implying that these two moieties are simply concatenated, C-terminal of the first connected to N-terminal of the second. The GFP moiety is circularly permuted (cpGFP), as in GCaMP sensors for Ca^{2+}. The circularly permuted cpGFP is then inserted into the PBP sequence, near the hinge region. Recently, the iNicSnFR project was aided by adding computational predictions[93–95] to the directed evolution pipeline. iNicSnFR12 achieves nearly the desired sensitivity in 96-well saline-based lab tests (Figure 2C).[86] The concentration–response relation is linear in the range shown, because the EC_{50} for the entire relation is >1 μM.[86]

The iNicSnFR approach exploits the amplification produced by modulating the fluorescence on the basis of nicotine binding to the PBP moiety. During each second that the single nicotine molecule is bound to the PBP, the fluorophore absorbs as many as 10^8 blue photons, then emits ~0.7 times as many green photons.[86] The optical elements resemble those of a modern fluorescence microscope, simplified further by measuring with a single photodetector ("fiber photometry"). Figure 3 presents a schematic for our planned next-generation CNM.

We presented preliminary data for an approach in which the purified iNicSnFR molecules are trapped within a hydrogel, at the tip of a fiber optic.[96] The hydrogel would be surrounded by ISF. The hydrogel approach (1) prevents other proteins from interacting with sensor molecules, distorting F_0 or ΔF, (2) avoids increasing F_0 by endogenous cellular fluorescence, and (3) minimizes contact with immune cells. The purified protein-hydrogel approach differs from most cpGFP sensors, which are expressed in animal models via viral vectors or transgenes. Points (1) and (2) also allow us to plan ways for absolute calibrations of δ-slope (see Figure 2C).

The Redox-Modified PBP Method

This method (Figure 4A) was suggested as early as 2001,[97] then lay fallow until 2021. A recent report confirmed the concept, for continuously sensing glutamine with the eponymously named glutamine binding protein.[98]

Site-selective modification would attach the redox probe to the nicotine-binding PBP at a sequence position that experiences an acceptably large movement (10–20 Å) upon ligand binding (see Figures 2B and 4A). We have defined several candidate residues, based on liganded and unliganded structures of iNicSnFR12. The original previous study, with other ligand–PBP pairs, coupled redox-active groups to introduced cysteine residues[97,98]; and we have begun with this tactic. Our preliminary experiments have utilized Cys variants of iNicSnFR12 and also the PBP alone, without the cpGFP moiety ("PBP12").

For the redox probe, one can choose among more than a dozen molecules.[99] We have begun experiments with methylene blue. Phenazine derivatives[98] and ruthenium (Ru(II))[97] have also been used with PBPs. In the most general tactic, one would site-selectively introduce noncanonical azido amino acids. Our preliminary studies have produced signals that show dose dependence on nicotine. However, we are still experimenting with conditions that yield satisfactory control data and also yield reversibility suitable for continuous sensing.

The electrodes for the intradermal version of the electrochemical CNM would be subcutaneous gold wires (0.5 mm diameter, 5 mm length) resembling those in CGMs—though with the more sophisticated analog processing required by pulsed techniques such as square-wave voltammetry. In another variation, the PBP could be coupled to a graphene monolayer that acts as the gate of a field-effect transistor.[100]

The PBP-Gated Nanopore Approach

A single nicotine binding event could, in principle, be amplified electrically if the binding gates a channel or a nanopore that passes 10^8 ions/s (a typical single-channel current) while the nicotine is bound (Figure 4B).[101,102] In a pioneering report, *Salmonella typhi* nanopores were embedded in planar bilayers. Conventional electrophysiological amplifiers and software were used in single-channel mode to analyze the nanopore current. Each of 13 different metabolite-binding PBPs proved suitable for ligand detection.[103] These were expressed in bacterial systems, purified, and added to the chambers separated by the membrane. The PBPs produced a range of fluctuations in the nanopore current, typically on a time scale of seconds. Adding the cognate ligand for the PBP then produced additional current fluctuations. Usually

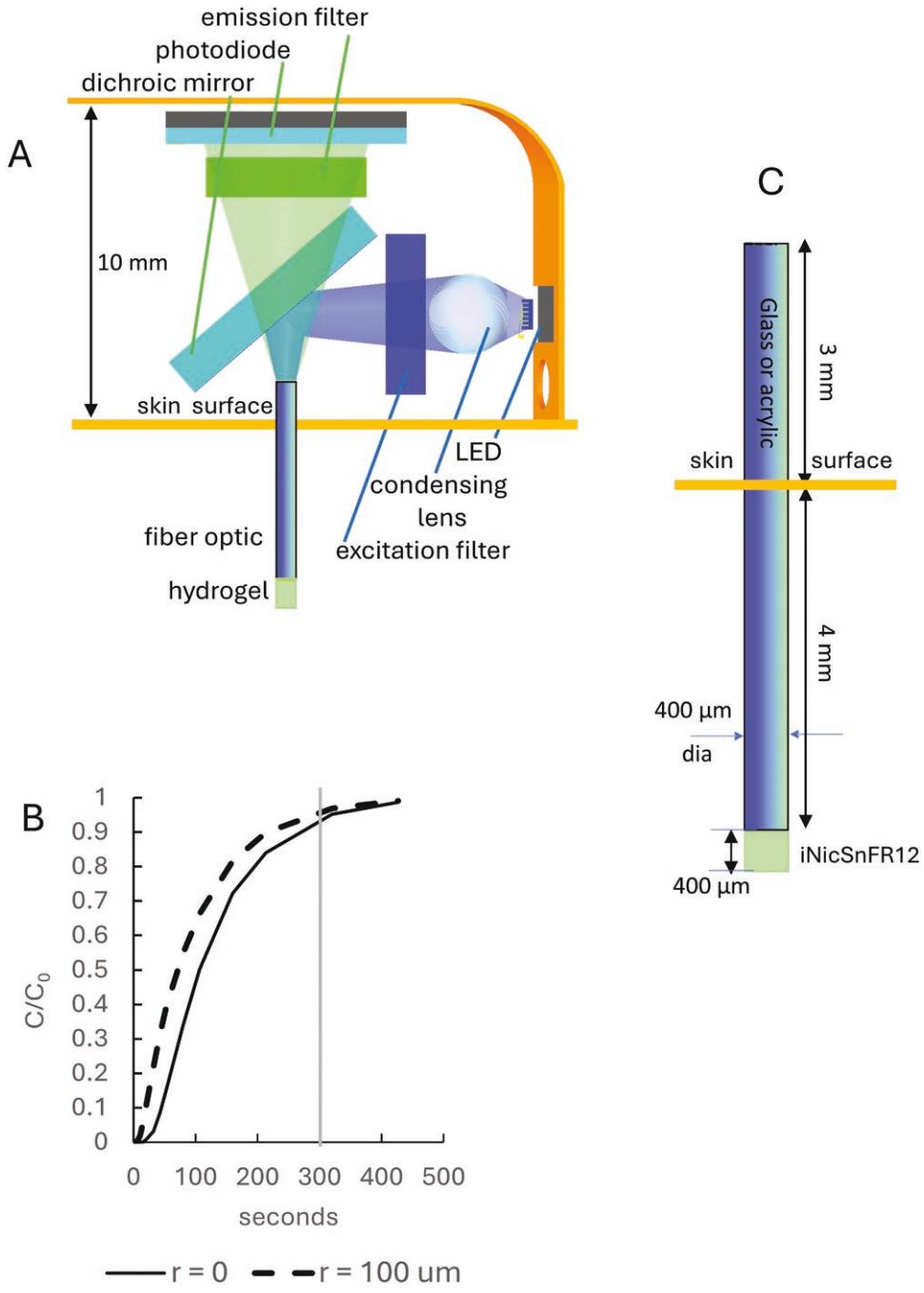

Figure 3. Design for a miniaturized fiber photometric CNM, based on initial progress with iNicSnFR12 entrapped in a hydrogel.[96] A, The iNicSnFR-containing hydrogel is placed in ISF, at the end of a fiber optic inserted by a spring apparatus like those in some CGMs.[120] The miniature fiber photometer is 14 mm tall, including the protruding fiber optic. There are two time-multiplexed excitation LEDs. Excitation at 470 and 405 nm yield nicotine-dependent and nicotine-insensitive fluorescence, respectively,[42,121] a common tactic to control for movement artifacts and bleaching. The SolidWorks file is available from the authors. B, Simulations of radial diffusion in a cylindrical hydrogel.[122,123] A hydrogel 400 µm in diameter contains 20 µM iNicSnFR. We assume that nicotine has a diffusion constant, D, of 0.3 µm²/ms in the hydrogel containing no iNicSnFR (~2/3 of the free-solution D). Effective D is further reduced by rebinding to iNicSnFR molecules with a K_d of 10 µM. Following a jump from [nicotine] = 0 to C_0 at time 0 in the external solution, $[nicotine]_t$ within the gel approaches 90% of C_0 within 300 s, satisfying the criterion for temporal resolution. C, In the design, the hydrogel contains 6.28 pmol of iNicSnFR, 20 µM. This is close to the 10 pmol of our standard assay condition in which a 100 µL microtiter well contains 100 nM iNicSnFR12 (see Figure 2). CGM = continuous glucose monitor; CNM = continuous nicotine monitor; iNicSnFR = intensity-based nicotine-sensing fluorescent reporter; ISF = interstitial fluid.

the liganded ("closed") conformation of the PBP blocked the current more completely, suggesting that "as the structure of the protein becomes more compacted, the protein penetrates deeper inside the nanopore, resulting in more current being blocked." Importantly, the EC_{50} of the ligand-induced current fluctuations was similar in all cases to the ligand–PBP interaction in solution.

Thus, the PBP-gated nanopore approach is biophysically tractable and pharmacologically understandable. Although no PBP was studied in the class F family which contains

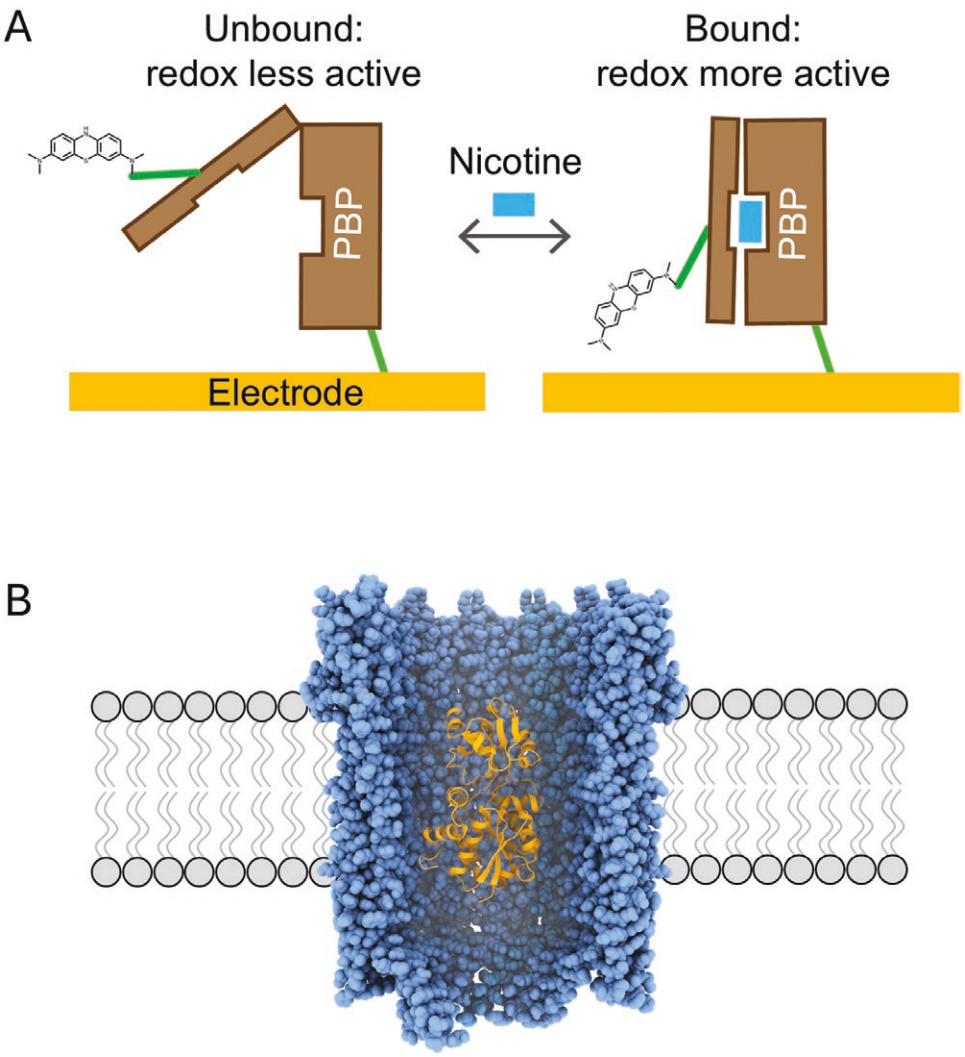

Figure 4. Electrochemical approaches to a CNM. A, PBP bearing a redox group. The exemplar group is methylene blue. B, Conceptual view of a PBP in a nanopore. The apo-PBP from iNiCSnFR3a (excised from pdb file 7S7W) was manually positioned within the vestibule of hemolysin E from *E. Coli K12* (pdb 2WCD), using ChimeraX. The complex was conceptually positioned in a bilayer membrane. CNM = continuous nicotine monitor; iNicSnFR = intensity-based nicotine-sensing fluorescent reporter; PBP = periplasmic binding protein.

OpuBC (the molecule that was evolved to yield PBP12),[91] these data are encouraging.

A deployable CNM need not be constrained by fragile lipid bilayers and single-channel measurements. The membrane would be a synthetic polymer, as used in pore sequencing; and many PBP12–nanopore complexes would be embedded in parallel, providing a macroscopic signal proportional to $[nicotine]_t$. This would utilize presently available high-throughput planar electrophysiological methods, for assaying candidate variants in a protein engineering campaign that develops and optimizes the PBP–nanopore complex. The supported membrane and electrodes would then be fixed to the tip of CGM-like probe.

Nicotine-Binding Aptamer-Based Approaches

In the present context, an aptamer (a synthetic single-stranded oligonucleotide) would be attached to an electrode. The aptamer would be evolved or selected to bind a nicotine molecule, changing shape. This would change the distance between an attached redox-active group and the electrode, resulting in a signal analogous to the redox-modified PBP.[104] Electrochemical aptamer-based sensors have been developed for metabolites, therapeutic drugs, and abused drugs; but unfortunately, there is not yet a reported aptamer with selective affinity for nicotine. Furthermore, we expect a poorer dynamic range and lifetime from aptamers compared to fluorescent hydrogels.[105]

Nicotine-Oxidizing Enzymes

In part because amperometric glucose sensors have found widespread use, investigators have considered oxidoreductase enzymes that already use nicotine as a substrate. The major challenge arises because we have specified that $[nicotine]_t$ must be measured at 10^6-fold lower levels than $[glucose]_t$, and each nicotine molecule that becomes oxidized by the enzyme contributes only a single elementary charge to the current.

Nicotine oxidase from *Pseudomonas putida* NicA2, was studied with amperometry.[106] Selectivity for nicotine is excellent. A mutated version became the basis for an issued patent,[107] aimed primarily at measurements in sweat. The

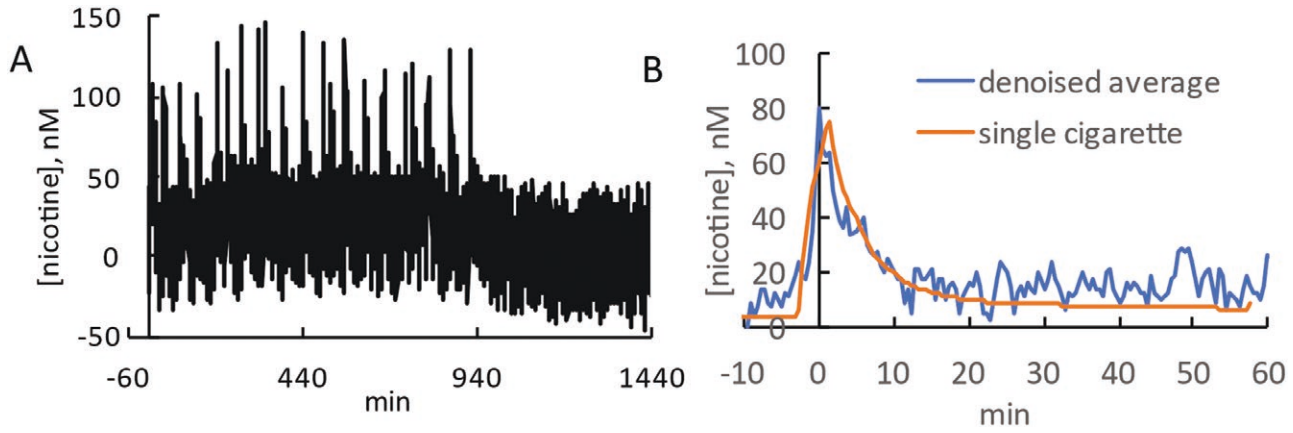

Figure 5. Synchronized averaging will reduce noise in CNM recordings. A, A simulated noisy CNM data stream. The dose table for the simulator[72] contained observed ad libitum times for one smoker[124] (21 cigarettes, total; we assumed 1 mg doses). We added white noise, single-pole filtered at $\tau = 5$ min (the target temporal resolution) with an RMS deviation of 29 nM (roughly the present resolution of iNicSnFR12). The resulting *[nicotine]*$_t$ signal is poorly discernible. B, Using the dose table, we retrospectively synchronized and averaged the traces during 10 min before and 60 min following the beginning of each cigarette. As expected, this decreased the noise by a factor $\sqrt{21}$. The resulting denoised average trace approximates the peak and waveform of the noiseless simulated *[nicotine]*$_t$ for a single cigarette. CNM = continuous nicotine monitor; iNicSnFR = intensity-based nicotine-sensing fluorescent reporter; RMS = root mean square.

Figure 6. A cartoon summary of this review's stated motivation for a measurements of individual [*nicotine*]$_t$, our present opinions on the most likely

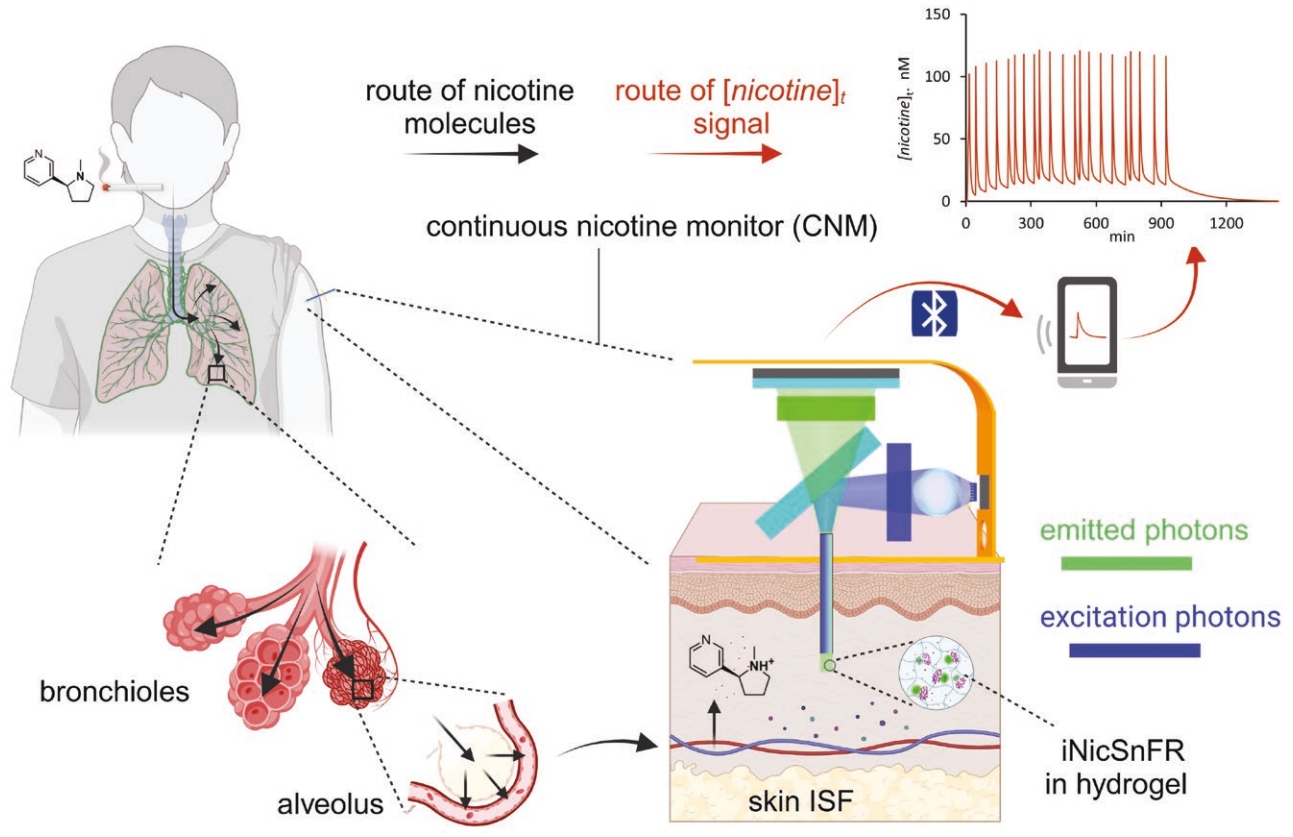

path to achieve a wearable CNM, and our suggestions for further analysis of [*nicotine*]$_t$. The lungs, especially the bronchioles and alveoli, are the most frequent route for nicotine to reach the bloodstream. Because ISF [*nicotine*]$_t$ strongly resembles blood and cerebrospinal fluid (CSF) [*nicotine*]$_t$ (see text), a minimally invasive intradermal CNM provides appropriate measurements of [*nicotine*]$_t$. Entrapping a purified protein of the iNicSnFR family in a hydrogel has promise as a molecular sensing strategy with the stated specifications. During ad libitum smoking or vaping, a photometric CNM can also incorporate compensation and normalization algorithms (not shown in detail) to result in the [*nicotine*]$_t$ signal. The wearable CNM communicates [*nicotine*]$_t$ via Bluetooth to a portable device. The [*nicotine*]$_t$ trace shown is simulated from the smoking times observed for ad libitum smoking by one exemplar subject over the time course of one day.[124,125] In the future, further time series analysis of many actual individual [*nicotine*]$_t$ records can enlighten research on nicotine and tobacco. Created partially in https://BioRender.com. CNM = continuous nicotine monitor; iNicSnFR = intensity-based nicotine-sensing fluorescent reporter.

limit of detection was 1 µM, yielding a current of 0.01 µA for an electrode area that was probably 3 mm^2. An intradermal electrode would presumably have a 100-fold smaller area. This would give a signal to 10 nM nicotine of just 1 pA, a challenge to measure. Studies on *Shinella* sp. *HZN7* NctB, another nicotine-oxidizing enzyme, show that mutations can increase turnover number only ~2-fold from the wild-type enzyme.[108]

The study of Tai et al.[81] claimed to measure the current associated with CYP2B6 oxidation of nicotine.[109] There was no control for the additional oxidative currents; it is likely that the enzyme simply increased previously measured faradaic currents[109] by ~2-fold, leaving the sensitivity at ~100-fold less than our goals.

Data Analysis

Pioneering instruments generally produce suboptimal data. It may not be possible for a CNM to detect when a subject takes a puff or otherwise ingests nicotine. We plan to equip the initial iNicSnFR12-based CNMs with three pushbuttons. Buttons 1, 2, and 3 "time-stamp" the signal at the beginning of a cigarette, a vaping session, or a nicotine pouch, respectively. In simulations, vast reductions in noise can result (Figure 5).

It would be desirable to automatically detect smoking/vaping episodes, so that subjects can ingest ad libitum without the added burden of time-stamping the dataset.[110] Machine leaning algorithms are being developed to identify meal times and predict individual patients' glucose trajectory from present CGM measurements.[110,111] How much of this effort is useful for the 24-hour measurements we envision for the CNM? We suggest that ~500 subject-days could provide an initial time-stamped dataset analogous to the glucose sensor time series in the OhioT1DM dataset, which contain 56 days × 8 type 1 diabetic patients.[112] This dataset could then provide a benchmark for developing new smoothing and curve-fitting algorithms.

The Caltech authors include a group with expertise in developing wearable devices. Like several other groups, we have reported on-device analog and digital signal processing, Bluetooth-based wireless communication, and battery power. These seem suitable for a CNM.[113,114]

A Not-for-Profit, Collaborative Research Agenda: Summary, Economics, and Support

Figure 6 summarizes this review in a cartoon form. Developing a CNM is a research agenda; and the outcome will be primarily a wearable instrument for research on the neuroscience of human nicotine use.

The example we have given, PATH-like research programs, might call for 30 000 CNMs/year. At these quantities, in the design of Figure 3, each thin-film wafer would be cut to yield 75 optical components (excitation filter, dichroic mirror, or emission filter). The total cost of these three components would be ~$18 per CNM. The electronics, including a Bluetooth chip with sufficient processing power to normalize and correct the signal, would cost ~$22 per CNM. Other components, including purified iNicSnFR protein, plastic fiber optic, lens, 3D-printed body, and battery, would have a total cost of ~$20. Therefore, we envision a cost of <$100 per CNM. If each subject in a PATH-like study wears a CNM for 24 hours in association with each annual interview, the additional cost will be $3 M/year—a single-digit percentage of the PATH budget.

We advocate a research agenda analogous to the ongoing, highly collaborative, international development of two other neuroscience instruments: miniature fluorescent microscopes[115] and high-density multielectrode probes.[116] Initial experiments can and must use rodent models; but unlike the two examples given, the research agenda must progress to measurements in humans with all deliberate speed. The medical device industry is largely driven by clinician uptake and insurance reimbursement; however, no reimbursement path for a CNM exists today. Therefore, the tobacco control, smoking cessation, and regulatory communities must decide whether public sources or a nonprofit startup[117] provide the most appropriate route for supporting the development of a CNM.

Supplementary Material

Supplementary material is available at *Nicotine and Tobacco Research* online.

References (101–125) are available as Supplementary Material.

Acknowledgments

H.A.L. thanks the Society for Research on Nicotine and Tobacco for the invitation to prepare this material for the 2024 Langley Lecture. We thank Mario Danek, Eric Donny, Ryan Drenan, Jed Rose, Rachel Tyndale, and Mitchell Zeller for helpful discussions. The Environmental Exposure and Toxicology Study Section of the California Tobacco-Related Disease Research Program (TRDRP) and the Neurobiology of Motivated Behavior Study Section of the National Institutes of Health provided written critiques of the motivation for a continuous nicotine monitor.

Funding

H.A.L. was supported by TRDRP Grant 27IP-0057, National Institute on Drug Abuse (NIDA) Grant DA049140, and National Institute of General Medical Sciences (NIGMS) Grant GM-123582. N.L.B. is supported National Institute on Drug Abuse (NIDA) Grant DA039264. N.J.F. was supported by the Biotechnology Leadership Program through the Rosen Bioengineering Center at Caltech. D.A.D., H.A.L., H.L., S.L.M., A.K.M., and W. G. were supported by internal Caltech grants from the Merkin Institute for Translational Research, the Rosen Biotechnology Center, the Carver Mead New Adventures Fund, and the Sensing to Intelligence Fund.

Declaration of Interests

Dr. Benowitz is a consultant to Achieve Life Sciences and Qnovia, companies that are developing smoking cessation medications, and has been a expert witness in litigation against tobacco companies. This review was written without active participation or encouragement by any person associated with the Population Assessment of Tobacco Health (PATH). The references to PATH exemplify the type of study that could complement use of a continuous nicotine monitor for understanding $[nicotine]_t$ during ad libitum nicotine intake. Dr. Wei Gao is co-founder and advisor at Persperity Health. Healther Lukas is an employee at Persperity Health.

Author Contributions

Aaron Nichols (Funding acquisition [equal], Investigation [equal], Writing—review & editing [equal]), Christopher Marotta (Investigation [equal], Writing—original draft [equal]), Heather Lukas (Investigation [equal], Writing—review & editing [equal]), Nicholas Friesenhahn (Investigation [equal]), Daniel Wagenaar (Conceptualization [equal], Software [equal]), Stephen Mayo (Conceptualization [equal], Funding acquisition [equal]), Dennis Dougherty (Conceptualization [equal], Supervision [equal]), Neal Benowitz (Conceptualization [equal], Funding acquisition [equal], Writing—review & editing [equal]), Wei Gao (Conceptualization [equal], Supervision [equal]), Anand Muthusamy (Conceptualization [equal], Writing—original draft [equal], Writing—review & editing [equal]), and Henry Lester (Conceptualization [equal], Funding acquisition [equal], Software [equal], Writing—original draft [equal])

References

1. Bowen A, Xing C, Inventors; 2015. Nicotine salt formulations for aerosol devices and methods thereof. *US patent 9,215,895*.
2. Brossard P, Weitkunat R, Poux V, *et al*. Nicotine pharmacokinetic profiles of the Tobacco Heating System 2.2, cigarettes and nicotine gum in Japanese smokers. *Regul Toxicol Pharmacol*. 2017;89:193–199.
3. Henningfield JE, Stapleton JM, Benowitz NL, Grayson RF, London ED. Higher levels of nicotine in arterial than in venous blood after cigarette smoking. *Drug Alcohol Depend*. 1993;33(1):23–29.
4. Rose JE, Behm FM, Westman EC, Coleman RE. Arterial nicotine kinetics during cigarette smoking and intravenous nicotine administration: implications for addiction. *Drug Alcohol Depend*. 1999;56(2):99–107.
5. Hukkanen J, Jacob P, 3rd, Benowitz NL. Metabolism and disposition kinetics of nicotine. *Pharmacol Rev*. 2005;57(1):79–115.
6. Wall A, Roslin S, Borg B, *et al*. E-cigarette aerosol deposition and disposition of [^{11}]nicotine using positron emission tomography: a comparison of nicotine uptake in lungs and brain using two different nicotine formulations. *Pharmaceuticals (Basel)*. 2022;15(3):367.
7. Henderson BJ, Lester HA. Inside-out neuropharmacology of nicotinic drugs. *Neuropharmacology*. 2015;96(Pt B):178–193.
8. Kovar L, Selzer D, Britz H, *et al*. Comprehensive parent-metabolite PBPK/PD modeling insights into nicotine replacement therapy strategies. *Clin Pharmacokinet*. 2020;59(9):1119–1134.
9. Alsharari SD, King JR, Nordman JC, *et al*. Effects of menthol on nicotine pharmacokinetic, pharmacology and dependence in mice. *PLoS One*. 2015;10(9):e0137070.
10. Benowitz NL, Herrera B, Jacob P, 3rd. Mentholated cigarette smoking inhibits nicotine metabolism. *J Pharmacol Exp Ther*. 2004;310(3):1208–1215.
11. Henderson BJ, Wall TR, Henley BM, *et al*. Menthol alone upregulates midbrain nAChRs, alters nAChR subtype stoichiometry, alters dopamine neuron firing frequency, and prevents nicotine reward. *J Neurosci*. 2016;36(10):2957–2974.
12. Brody A, Mukhin A, La Charite J, *et al*. Up-regulation of nicotinic acetylcholine receptors in menthol cigarette smokers. *Int J Neuropsychopharmacol*. 2013;16(5):957–966.
13. Benowitz NL, Hukkanen J, Jacob P, 3rd. Nicotine chemistry, metabolism, kinetics and biomarkers. *Handb Exp Pharmacol*. 2009(192):29–60. doi: 10.1007/978-3-540-69248-5_2
14. Schreiner BS, Lehmann R, Thiel U, *et al*. Direct action and modulating effect of (+)- and (-)-nicotine on ion channels expressed in trigeminal sensory neurons. *Eur J Pharmacol*. 2014;728:48–58. doi:10.1016/j.ejphar.2014.01.060
15. Maher EE, Strzelecki AM, Weafer JJ, Gipson CD. The importance of translationally evaluating steroid hormone contributions to substance use. *Front Neuroendocrinol*. 2023;69:101059. doi:10.1016/j.yfrne.2023.101059
16. Klemperer EM, Kock L, Feinstein MJP, *et al*. Sex differences in tobacco use, attempts to quit smoking, and cessation among dual users of cigarettes and e-cigarettes: longitudinal findings from the US Population Assessment of Tobacco and Health study. *Prev Med*. 2024;185:108024. doi:10.1016/j.ypmed.2024
17. McKee SA, McRae-Clark AL. Consideration of sex and gender differences in addiction medication response. *Biol Sex Differ*. 2022;13(1):34.
18. Benowitz NL, Lessov-Schlaggar CN, Swan GE, Jacob P, 3rd. Female sex and oral contraceptive use accelerate nicotine metabolism. *Clin Pharmacol Ther*. 2006;79(5):480–488.
19. Ren M, Lotfipour S, Leslie F. Unique effects of nicotine across the lifespan. *Pharmacol Biochem Behav*. 2022;214:173343. doi:10.1016/j.pbb.2022.173343
20. Perez-Martin H, Lidon-Moyano C, Gonzalez-Marron A, *et al*. Variation in nicotine metabolization according to biological factors and type of nicotine consumer. *Healthcare (Basel)*. 2023;11(2):179.
21. Molander L, Hansson A, Lunell E. Pharmacokinetics of nicotine in healthy elderly people. *Clin Pharmacol Ther*. 2001;69(1):57–65.
22. Benowitz NL, Donny EC, Edwards KC, Hatsukami D, Smith TT. The role of compensation in nicotine reduction. *Nicotine Tob Res*. 2019;21(Suppl 1):S16–S18.
23. Krebs NM, Zhu J, Wasserman E, *et al*. Switching to progressively reduced nicotine content cigarettes in smokers with low socioeconomic status: a double-blind randomized clinical trial. *Nicotine Tob Res*. 2021;23(6):992–1001.
24. Hatsukami DK, Luo X, Jensen JA, *et al*. Effect of immediate vs gradual reduction in nicotine content of cigarettes on biomarkers of smoke exposure: a randomized clinical trial. *J Am Med Assoc*. 2018;320(9):880–891.
25. Cox S, Goniewicz ML, Kosmider L, *et al*. The time course of compensatory puffing with an electronic cigarette: secondary analysis of real-world puffing data with high and low nicotine concentration under fixed and adjustable power settings. *Nicotine Tob Res*. 2021;23(7):1153–1159.
26. Glantz SA, Nguyen N, Oliveira da Silva AL. Population-based disease odds for E-cigarettes and dual use versus cigarettes. *NEJM Evid*. 2024;3(3):EVIDoa2300229.
27. Gottlieb S, Zeller M. A nicotine-focused framework for public health. *N Engl J Med*. 2017;377(12):1111–1114.
28. Fink JB, Stapleton KW. Nebulizers. *J Aerosol Med Pulm Drug Deliv*. 2024;37(3):140–156.
29. Knoch M. New generation nebulizers. *J Aerosol Med Pulm Drug Deliv*. 2024;37(3):157–165.
30. Danek M, Inventor; 2021. Apparatus for producing an aerosol for inhalation by a person. US patent US 10,888,117 B2.
31. Danek M, Inventor; 2024. Apparatus for producing an aerosol for inhalation by a person. *US patent US11690963B2*.
32. Danek M, Betts K, Kovacevich I, *et al*., Inventors; 2024. Electronic devices for aerosolizing and inhaling liquid having diaphragm and a pressure sensor. *US patent US11925207B2*.
33. Businesswire. *Qnovia, Inc. Announces Positive Results from First-in-Human Pharmacokinetic and Safety Study of Lead Asset QN-01, a Prescription Inhaled Smoking Cessation Therapy*. 2023; https://www.businesswire.com/news/home/20231129757219/en/. Accessed October 1, 2024.
34. El Hourani M, Shihadeh A, Talih S, Eissenberg T; CSTP Nicotine Flux Work Group. Comparison of nicotine emissions rate, 'nicotine flux', from heated, electronic and combustible tobacco products: data, trends and recommendations for regulation. *Tob Control*. 2023;32:e180–e183. doi:10.1136/tobaccocontrol-2021-056850
35. Kolli AR, Veljkovic E, Calvino-Martin F, *et al*. Nicotine flux and pharmacokinetics-based considerations for early assessment of nicotine delivery systems. *Drug Alcohol Depend Rep*. 2024;11:100245. doi:10.1016/j.dadr.2024.100245

36. Williams JM, Foulds J. *Treating Addiction to Tobacco and Nicotine Products*. 2025. ISBN 978-1-61537-468-7.
37. Marks MJ, Stitzel JA, Collins AC. Time course study of the effects of chronic nicotine infusion on drug response and brain receptors. *J Pharmacol Exp Ther.* 1985;235(3):619–628.
38. Schwartz RD, Kellar KJ. In vivo regulation of [^{3}H]acetylcholine recognition sites in brain by nicotinic cholinergic drugs. *J Neurochem.* 1985;45(2):427–433.
39. Bencherif M, Fowler K, Lukas RJ, Lippiello PM. Mechanisms of up-regulation of neuronal nicotinic acetylcholine receptors in clonal cell lines and primary cultures of fetal rat brain. *J Pharmacol Exp Ther.* 1995;275(2):987–994.
40. Kuryatov A, Luo J, Cooper J, Lindstrom J. Nicotine acts as a pharmacological chaperone to up-regulate human α4β2 acetylcholine receptors. *Mol Pharmacol.* 2005;68(6):1839–1851.
41. Nashmi R, Xiao C, Deshpande P, *et al.* Chronic nicotine cell specifically upregulates functional α4* nicotinic receptors: basis for both tolerance in midbrain and enhanced long-term potentiation in perforant path. *J Neurosci.* 2007;27(31):8202-8218.
42. Shivange AV, Borden PM, Muthusamy AK, *et al*. Determining the pharmacokinetics of nicotinic drugs in the endoplasmic reticulum using biosensors. *J Gen Physiol.* 2019;151(4):738–757.
43. Benowitz NL, Jacob P, 3rd, Denaro C, Jenkins R. Stable isotope studies of nicotine kinetics and bioavailability. *Clin Pharmacol Ther.* 1991;49(3):270–277.
44. Levi M, Dempsey DA, Benowitz NL, Sheiner LB. Population pharmacokinetics of nicotine and its metabolites I. Model development. *J Pharmacokinet Pharmacodyn.* 2007;34(1):5–21.
45. Teeguarden JG, Housand CJ, Smith JN, *et al*. A multi-route model of nicotine-cotinine pharmacokinetics, pharmacodynamics and brain nicotinic acetylcholine receptor binding in humans. *Regul Toxicol Pharmacol.* 2013;65(1):12–28.
46. Marchand M, Brossard P, Merdjan H, *et al*. Nicotine population pharmacokinetics in healthy adult smokers: a retrospective analysis. *Eur J Drug Metab Pharmacokinet*. 2017;42(6):943–954.
47. Matta SG, Balfour DJ, Benowitz NL, *et al*. Guidelines on nicotine dose selection for in vivo research. *Psychopharmacology (Berl)*. 2007;190(3):269–319.
48. Hansen E, Arendt-Nielsen L, Boudreau SA. A comparison of oral sensory effects of three TRPA1 agonists in young adult smokers and non-smokers. *Front Physiol.* 2017;8:663. doi:10.3389/fphys.2017.00663
49. Carstens E, Carstens MI. Sensory effects of nicotine and tobacco. *Nicotine Tob Res*. 2022;24(3):306–315.
50. Fu XW, Lindstrom J, Spindel ER. Nicotine activates and up-regulates nicotinic acetylcholine receptors in bronchial epithelial cells. *Am J Respir Cell Mol Biol.* 2009;41(1):93–99.
51. Mazzo F, Pistillo F, Grazioso G, *et al*. Nicotine-modulated subunit stoichiometry affects stability and trafficking of α3β4 nicotinic receptor. *J Neurosci*. 2013;33(30):12316–12328.
52. Claw KG, Beans JA, Lee SB, *et al*. Pharmacogenomics of nicotine metabolism: novel CYP2A6 and CYP2B6 genetic variation patterns in Alaska Native and American Indian populations. *Nicotine Tob Res*. 2019;22(6):910–918.
53. Howard LA, Ahluwalia JS, Lin SK, Sellers EM, Tyndale RF. CYP2E1*1D regulatory polymorphism: association with alcohol and nicotine dependence. *Pharmacogenetics*. 2003;13(6):321–328.
54. Cao Y, Liu X, Hu Z, *et al*. Assessing nicotine pharmacokinetics of new generation tobacco products and conventional cigarettes: a systematic review and meta-analysis. *Nicotine Tob Res*. 2024.
55. Benowitz NL, Jacob P, 3rd. Metabolism of nicotine to cotinine studied by a dual stable isotope method. *Clin Pharmacol Ther.* 1994;56(5):483–493.
56. Yingst JM, Foulds J, Veldheer S, *et al*. Nicotine absorption during electronic cigarette use among regular users. *PLoS One*. 2019;14(7):e0220300.
57. Yingst JM, Hrabovsky S, Hobkirk A, *et al*. Nicotine absorption profile among regular users of a pod-based electronic nicotine delivery system. *JAMA Netw Open*. 2019;2(11):e1915494.
58. Solingapuram Sai KK, Zuo Y, Rose JE, *et al*. Rapid brain nicotine uptake from electronic cigarettes. *J Nucl Med.* 2020;61(6):928–930.
59. Zuo Y, Mukhin AG, Berg H, *et al*. Comparison of brain nicotine uptake from electronic cigarettes and combustible cigarettes. *Neuropsychopharmacology.* 2022;47(11):1939–1944.
60. Dempsey D, Tutka P, Jacob P, 3rd, *et al*. Nicotine metabolite ratio as an index of cytochrome P450 2A6 metabolic activity. *Clin Pharmacol Ther.* 2004;76(1):64–72.
61. Tanner JA, Tyndale RF. Variation in CYP2A6 activity and personalized medicine. *J Pers Med*. 2017;7(4):18.
62. Chenoweth MJ, Lerman C, Knight J, Tyndale RF. Influence of CYP2A6 genetic variation, nicotine dependence severity, and treatment on smoking cessation success. *Nicotine Tob Res.* 2023;25(6):1207–1211.
63. El-Boraie A, Taghavi T, Chenoweth MJ, *et al*. Evaluation of a weighted genetic risk score for the prediction of biomarkers of CYP2A6 activity. *Addict Biol.* 2020;25(1):e12741.
64. Benowitz NL. Cigarette smoking and cardiovascular disease: pathophysiology and implications for treatment. *Prog Cardiovasc Dis.* 2003;46(1):91–111.
65. St Helen G, Ross KC, Dempsey DA, *et al*. Nicotine delivery and vaping behavior during ad libitum E-cigarette access. *Tob Regul Sci*. 2016;2(4):363–376.
66. Mendelson JH, Goletiani N, Sholar MB, Siegel AJ, Mello NK. Effects of smoking successive low- and high-nicotine cigarettes on hypothalamic-pituitary-adrenal axis hormones and mood in men. *Neuropsychopharmacology.* 2008;33(4):749–760.
67. Pauwels CGGM, Boots AW, Visser WF, *et al*. Characteristic human individual puffing profiles can generate more TNCO than ISO and Health Canada regimes on smoking machine when the same brand is smoked. *Int J Environ Res Public Health*. 2020;17(9):erph3225.
68. Smith D, Allerton C, Kalgutkar A, van de Waterbeemd H, Walker D. *Pharmacokinetics and Metabolism in Drug Design*. 3rd ed. Weinheim, Germany: Wiley; 2012.
69. Olsson Gisleskog PO, Perez Ruixo JJ, Westin A, Hansson AC, Soons PA. Nicotine population pharmacokinetics in healthy smokers after intravenous, oral, buccal and transdermal administration. *Clin Pharmacokinet*. 2021;60(4):541–561.
70. NCBI. *PubChem Nicotine. CID=89594*. https://pubchem.ncbi.nlm.nih.gov/compound/89594. Accessed October 1, 2024.
71. Miwa JM, Freedman R, Lester HA. Neural systems governed by nicotinic acetylcholine receptors: emerging hypotheses. *Neuron.* 2011;70(1):20–33.
72. Wang AZ, Jeon J, Drenan RM. Boyukozturk F, Lester HA. Simulating early steps in nicotine dependence: pharmacokinetics, activation, and chaperoning of nicotinic receptors. *Mol Pharmacol.* 2025;107(4):100016.
73. Rollema H, Shrikhande A, Ward KM, *et al*. Pre-clinical properties of the α4β2 nicotinic acetylcholine receptor partial agonists varenicline, cytisine and dianicline translate to clinical efficacy for nicotine dependence. *Br J Pharmacol.* 2010;160(2):334–345.
74. Pankow JF. A consideration of the role of gas/particle partitioning in the deposition of nicotine and other tobacco smoke compounds in the respiratory tract. *Chem Res Toxicol.* 2001;14(11):1465–1481.
75. Benowitz NL. The central role of pH in the clinical pharmacology of nicotine: implications for abuse liability, cigarette harm reduction and FDA regulation. *Clin Pharmacol Ther.* 2022;111(5):1004–1006.
76. Zuo Y, Solingapuram Sai KK, Jazic A, *et al*. Comparison of brain nicotine accumulation from traditional combustible cigarettes and electronic cigarettes with different formulations. *Neuropsychopharmacology.* 2024;49(4):740–746.
77. Irace C, Cutruzzolà A, Tweden K, Kaufman FR. Device profile of the eversense continuous glucose monitoring system for glycemic control in type-1 diabetes: overview of its safety and efficacy. *Expert Rev Med Devices*. 2021;18(10):909–914.
78. Mortellaro M, DeHennis A. Performance characterization of an abiotic and fluorescent-based continuous glucose monitoring

system in patients with type 1 diabetes. *Biosens Bioelectron*. 2014;61:227–231.
79. Sonner Z, Wilder E, Heikenfeld J, *et al*. The microfluidics of the eccrine sweat gland, including biomarker partitioning, transport, and biosensing implications. *Biomicrofluidics*. 2015;9(3):031301.
80. Lin H, Tan J, Zhu J, *et al*. A programmable epidermal microfluidic valving system for wearable biofluid management and contextual biomarker analysis. *Nat Commun*. 2020;11(1):4405.
81. Tai LC, Ahn CH, Nyein HYY, *et al*. Nicotine monitoring with a wearable sweat band. *ACS Sensors*. 2020;5(6):1831–1837.
82. Min J, Tu J, Xu C, *et al*. Skin-interfaced wearable sweat sensors for precision medicine. *Chem Rev*. 2023;123(8):5049–5138.
83. Choi J, Chen S, Deng Y, *et al*. Skin-interfaced microfluidic systems that combine hard and soft materials for demanding applications in sweat capture and analysis. *Adv Healthc Mater*. 2021;10(4):e2000722.
84. Harshman SW, Strayer KE, Davidson CN, *et al*. Rate normalization for sweat metabolomics biomarker discovery. *Talanta*. 2021;223(Pt 1):121797.
85. Yang Y, Gao W. Wearable and flexible electronics for continuous molecular monitoring. *Chem Soc Rev*. 2019;48(6):1465–1491.
86. Haloi N, Huang S, Nichols AL, *et al*. Interactive computational and experimental approaches improve the sensitivity of periplasmic binding protein-based nicotine biosensors for measurements in biofluids. *Protein Eng Des Sel*. 2024;37.
87. Hoss U, Budiman ES. Factory-calibrated continuous glucose sensors: the science behind the technology. *Diabetes Technol Ther*. 2017;19(S2):S44–S50.
88. Gonzalez WG, Zhang H, Harutyunyan A, Lois C. Persistence of neuronal representations through time and damage in the hippocampus. *Science*. 2019;365(6455):821–825.
89. Muthusamy A, Rosenberg M, Kim C, *et al*. Correspondence of fentanyl brain pharmacokinetics and behavior measured via engineering opioids biosensors and computational ethology. *bioRxiv*. 2024:2024.2003.2015.584894, preprint: not peer reviewed. doi:10.1101/2024.03.15.584894
90. Nichols AL, Blumenfeld Z, Fan C, *et al*. Fluorescence activation mechanism and imaging of drug permeation with new sensors for smoking-cessation ligands. *eLife*. 2022;11:e74648.
91. Scheepers GH, Lycklama ANJA, Poolman B. An updated structural classification of substrate-binding proteins. *FEBS Lett*. 2016;590(23):4393–4401.
92. Borden P, Shivange AV, Marvin JS, *et al*. A genetically encoded fluorescent sensor for in vivo acetylcholine detection. *bioRxiv*, 2019. doi:10.1101/2020.02.07.939504
93. Unger EK, Keller JP, Altermatt M, *et al*. Directed evolution of a selective and sensitive serotonin sensor via machine learning. *Cell*. 2020;183(7):1986–2002.e26.
94. Privett HK, Kiss G, Lee TM, *et al*. Iterative approach to computational enzyme design. *Proc Natl Acad Sci USA*. 2012;109(10):3790–3795.
95. Blomberg R, Kries H, Pinkas DM, *et al*. Precision is essential for efficient catalysis in an evolved Kemp eliminase. *Nature*. 2013;503(7476):418–421.
96. Nichols AL, Marotta CB, Wagenaar DA, *et al*. Hydrogel encapsulation of a designed fluorescent protein biosensor for continuous measurements of sub-100 nanomolar nicotine. *bioRxiv*. 2024:2024.2012.2002.625538, preprint: not peer reviewed. doi:10.1101/2024.12.02.625538
97. Benson DE, Conrad DW, de Lorimier RM, Trammell SA, Hellinga HW. Design of bioelectronic interfaces by exploiting hinge-bending motions in proteins. *Science*. 2001;293(5535):1641–1644.
98. Takamatsu S, Lee J, Asano R, *et al*. Continuous electrochemical monitoring of L-glutamine using redox-probe-modified L-glutamine-binding protein based on intermittent pulse amperometry. *Sens Actuators B*. 2021;346:130554.
99. Kang D, Ricci F, White RJ, Plaxco KW. Survey of redox-active moieties for application in multiplexed electrochemical biosensors. *Anal Chem*. 2016;88(21):10452–10458.
100. Krishnan SK, Nataraj N, Meyyappan M, Pal U. Graphene-based field-effect transistors in biosensing and neural interfacing applications: recent advances and prospects. *Anal Chem*. 2023;95(5):2590–2622.